Title

Fabrication and thermal stability of arrays of Fe nanodots

Journal

Applied Physics Letters, 81(23)

Authors

Liu, Kai
Nogues, J.
Leighton, C.
et al.

Publication Date

2002-10-10

DOI

10.1063/1.1526458#

Peer reviewed

Fabrication and thermal stability of arrays of Fe nanodots

Kai Liu[a)]
Department of Physics, University of California–San Diego, La Jolla, California 92093-0319 and Department of Physics, University of California, Davis, California 95616

J. Nogués
Institució Catalana de Recerca i Estudis Avançats (ICREA) and Departament de Física, Universitat Autònoma de Barcelona, 08193 Bellaterra, Spain

C. Leighton
Department of Chemical Engineering and Materials Science, University of Minnesota, Minneapolis, Minnesota 55455

H. Masuda and K. Nishio
Applied Chemistry Department, Tokyo Metropolitan University, Hachioji, Tokyo 192-0397, Japan

I. V. Roshchin and Ivan K. Schuller
Department of Physics, University of California–San Diego, La Jolla, California 92093-0319

(Received 9 July 2002; accepted 10 October 2002)

We have fabricated arrays of 60-nm-size magnetic Fe nanodots over a 1-cm^2-size area using nanoporous alumina membranes as shadow masks. The size and size distribution of the nanodots correlate very well with that of the membrane pores. By placing an antiferromagnetic FeF_2 layer underneath the Fe nanodots, an exchange anisotropy can be introduced into the Fe/FeF_2 system. We have observed an increase in the magnetic hysteresis loop squareness in biased nanodots, suggesting that exchange bias may be used as a tunable source of anisotropy to stabilize the magnetization in such nanodots. © *2002 American Institute of Physics.* [DOI: 10.1063/1.1526458]

Magnetic nanostructures often exhibit interesting properties as the sample size becomes comparable to certain characteristic length scales, such as the spin–flip diffusion length and magnetic domain-wall width.[1,2] Technologically, these nanostructures are driving the device miniaturization (e.g., towards Tbit/in.^{2} data acquisition), as well as providing more functionality.[3] However, in practice, it becomes increasingly challenging to fabricate and characterize nanostructures with decreasing feature sizes, beyond the limit of conventional photolithography. Certain techniques have shown promise in mass-producing nanostructures cost effectively, such as extreme ultraviolet lithography, ion irradiation, nanoimprint, interferometry, nanotemplate, and self-assembly.[2,4–14] Another important issue is the thermal stability of these magnetic nanostructures, since the anisotropy energy that stabilizes the magnetization scales with the volume. At very small sizes, the magnetization direction is randomized by thermal fluctuations, posing a fundamental ''superparamagnetic limit'' to achievable magnetic recording density.[15–17] Several schemes have been proposed to postpone or circumvent the superparamagnetic limit.[5,12,15–19] In this work, we demonstrate a porous alumina shadow mask technique to realize nanomagnet arrays with a magnet size of about 60 nm over a 1 cm^2 area. We also show that exchange bias may be used as an additional and tunable means of anisotropy for magnetization stabilization in nanomagnets.

A schematic of the sample preparation process is shown in Fig. 1(a). A porous alumina membrane is first prepared by anodic oxidation of aluminum.[8,20] The oxidized film consists of packed columnar arrays of nanopores. The porous membrane is then separated from the aluminum metal by etching and transferred onto a substrate.[8,11] The subsequent material deposition through the alumina mask and the final lift-off lead to nanodot arrays.

In this study, 300-nm-thick alumina membranes have been used, with a 60 nm pore size and a $10^{10}/cm^2$ (~60 Gbit/in^2) pore density. A scanning electron microscope (SEM) image of the membrane transferred onto a MgO substrate is shown in Fig. 1(b). Using this membrane as a shadow mask, a 15-nm-thick Fe layer is deposited by electron-beam (e-beam) evaporation through the pores onto the substrate. The membrane is subsequently removed in a

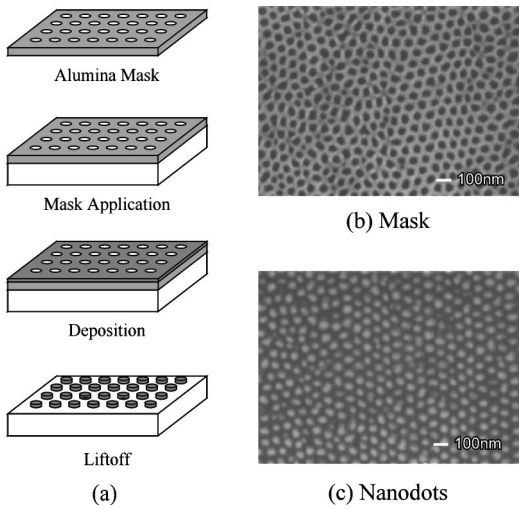

FIG. 1. (a) Schematic of the porous alumina shadow mask deposition technique. Top view, SEM images of (b) a porous alumina membrane and (c) arrays of Fe nanodots after the fabrication process.

a)Electronic mail: kailiu@ucdavis.edu

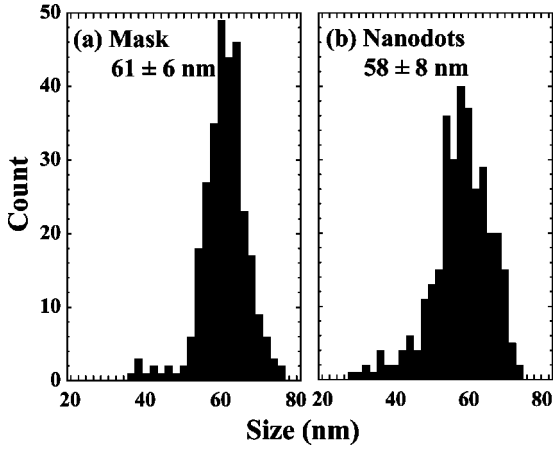

FIG. 2. Histograms of pore/dot size distribution of (a) the nanoporous alumina membrane and (b) arrays of Fe nanodots.

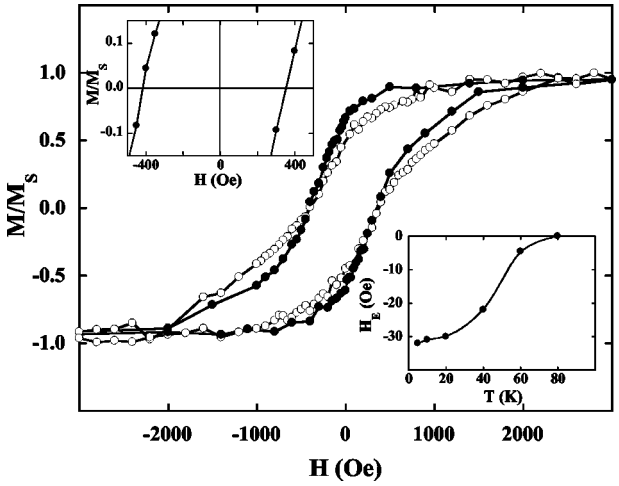

FIG. 3. Magnetic hysteresis loops of Fe nanodot arrays (60 nm wide, 15 nm thick) on MgO (unbiased, open symbols) and a 90-nm-thick FeF_2 film (exchange biased, solid symbols) at 10 K, after field cooling in 5 kOe from 300 K. The upper-left inset shows a section of the biased loop near zero field. The lower-right inset shows the temperature dependence of the exchange field for the biased Fe nanodots.

10% NaOH solution. This lift-off process leaves behind Fe nanodot arrays over about a 1 cm^2 area, as shown in Fig. 1(c). The pattern transfer from the mask to the nanodots is also illustrated in Fig. 2. From the SEM images [Figs. 1(b) and 1(c)], by digitizing the areas of the pores in the alumina mask and the Fe nanodots, we have determined the size distribution of the pores and nanodots, respectively.[21] In the alumina mask, the pores are fairly uniform in size, with an average diameter of 61 ± 6 nm [Fig. 2(a)]. In the Fe nanodots, the size, along with the narrow size distribution, is well maintained through the lift-off process. The average diameter of the dot is 58 ± 8 nm [Fig. 2(b)]. Indeed, the combination of a thin mask and a directional flux minimized any ''shadowing'' effect that could have compromised the structural integrity.

For comparison and consistency, three samples have been made on the same substrate in the following manner. A clean MgO(100) substrate is used and half of the area is covered by a 90-nm-thick antiferromagnetic FeF_2 layer through e-beam evaporation, while the other half remains bare. The FeF_2, grown at 0.2 nm/s and 200 °C, is a twinned quasiepitaxial layer along the (110) direction.[13,22,23] The alumina membrane is then applied on top of both halves, except a bar-shaped region on the bare MgO. The subsequent deposition of a 15-nm-thick Fe layer (at 0.1 nm/s and 150 °C) and the lift-off result in three types of samples on the same substrate: (1) 60-nm-size Fe nanodots (15 nm thick)/MgO; (2) 60-nm-size Fe nanodots (15 nm)/FeF_2 (90 nm)/MgO, and (3) Fe film (15 nm)/MgO. The exact growth conditions have been reported in earlier studies.[13,22,23] The Fe layer thus prepared is polycrystalline, and grows similarly on MgO and FeF_2.

The large area and high density of the nanodot arrays facilitate their characterization. In this study, all magnetic measurements have been performed in the in-plane geometry using a superconducting quantum interference device magnetometer. At 300 K, the uniform Fe film exhibits the usual square loop with a small coercivity H_C of 25 Oe. The squareness of the loop, defined as the ratio of remanent magnetization M_R over saturation magnetization M_S, is 84%. In contrast, the loop of the Fe nanodot arrays at 300 K is much more sheared with a larger H_C of 110 Oe and a smaller squareness of 15%. Primary contributions to the different loop shapes are the demagnetization field and, to a lesser degree, magnetic dipolar interactions between the dots.[24] Because of the polycrystalline nature of the Fe film and nanodots, contributions from magnetocrystalline anisotropy are negligible. The increased coercivity in Fe nanodots is a well-known phenomenon for fine magnetic particles.[25] The small dimension of the dots impedes the formation of multidomains and the magnetization reversal proceeds primarily through rotation. The small remanent magnetization of the Fe nanodots is an indication of the reduced anisotropy energy relative to the thermal fluctuations, given that the simultaneously made Fe nanodots and film on the same substrate should have similar structural characteristics. The anisotropy energy (product of anisotropy constant K and volume V) decreases as the nanodot becomes smaller, and the effects of thermal fluctuation become significant, eventually leading to superparamagnetism. Therefore, the remanent magnetization or squareness of the loop may be used as an indication of the thermal stability of the nanomagnets.

The exchange anisotropy in the ferromagnet/antiferromagnet (FM/AF) system is another *external* source for magnetization stabilization. When a FM/AF bilayer is field cooled across the AF Néel temperature T_N, an exchange anisotropy is frozen in. The FM magnetic hysteresis loop is shifted from the origin by an amount known as the exchange field H_E, which measures the exchange anisotropy strength.[26] It is noteworthy that exchange bias (EB) has been proposed theoretically to stabilize the magnetization in small particles.[27] Moreover, it has been shown experimentally that ball-milled FM particles embedded in an AF matrix exhibit improved squareness.[28]

For the sample with Fe nanodot arrays on top of an AF FeF_2 layer, the exchange anisotropy was introduced by field cooling the bilayer in a 5 kOe field from 300 K to below the FeF_2 T_N ($\sim$80 K). A resultant hysteresis loop at 10 K is shown in Fig. 3, shifted from zero field to the left by 31 Oe (better seen in the expanded view). The loop shift, or exchange field H_E, is easily measurable and it diminishes with

increasing temperature, eventually vanishing at the FeF_2 T_N (Fig. 3, inset). Notice that the magnitude of H_E is one order of magnitude smaller than that in uniform Fe/FeF_2 bilayer films.[22,23] This is due to the exposed FeF_2 surface during the alumina mask application process, resulting in a contaminated Fe/FeF_2 interface. It further attests to the interfacial nature of EB.

Even with the modest exchange bias, the remanent magnetization M_R and squareness of the hysteresis loop are improved. For example, at 10 K, the unbiased Fe nanodots show a M_R of 52% M_S (Fig. 3), due to the aforementioned demagnetization field, dipolar interactions, as well as thermal fluctuations. In comparison, the biased Fe nanodots grown on the same substrate show a magnetization of 64% M_S at the exchange field of -31 Oe, while at zero field the M_R is 67% and 61% of M_S in the decreasing- and increasing-field branches, respectively (Fig. 3). The improvement should be mainly attributed to the exchange anisotropy. We can estimate the exchange anisotropy energy per unit area[26] at 10 K as $H_E t M = 0.077$ erg/cm^2, where t is the Fe layer thickness. Over the 60-nm-size area of a nanodot, the anisotropy is about 1.35 eV, or about 1500 times the thermal energy at 10 K. Had the Fe/FeF_2 interface been cleaner, the stabilization effect would be even greater. Additionally, EB can be controlled by other parameters, such as constituent material, cooling field strength, crystallinity, etc., which can be used to control the magnetization stabilization.

In summary, we have fabricated arrays of Fe nanodots using a porous alumina shadow mask technique. The nanodots are 60 nm in size, realized over macroscopic areas. The masks used are mechanically stable, thus this technique is robust. Further improvements on the eccentricity of the individual dots, decreasing their size and dispersion are needed. We demonstrate that FM/AF exchange bias may be used as an additional and tunable source of anisotropy to stabilize the magnetization in these nanodots. These nanostructures also provide a model system to study the intricate physics in exchange biased FM/AF layers.

This work has been supported by the AFOSR, (F49620-01-0393) and in part by the U.C. Davis–New Faculty Research Grant, the Catalan DGR (2001SGR00189), and the NEXBIAS European Network (HPRN-CT-2002-00296). The authors thank O. Nakamura for establishing the contacts between UCSD and TMU.

[1] See, e.g., D. D. Awschalom and S. von Molnár, *Nanotechnology*, edited by G. Timp (Springer, New York, 1998), Chap. 12.
[2] J. I. Martin, J. Nogués, K. Liu, J. L. Vicent, and I. K. Schuller, J. Magn. Magn. Mater. (in press).
[3] S. A. Wolf, D. D. Awschalom, R. A. Burham, J. M. Daughton, S. von Molnár, M. L. Roukes, A. Y. Chtchelkanova, and D. M. Treger, Science **294**, 1488 (2001).
[4] R. H. Stulen and D. W. Sweeney, IEEE J. Quantum Electron. **35**, 694 (1999).
[5] B. D. Terris, L. Folks, D. Weller, J. E. E. Baglin, A. J. Kellock, H. Rothuizen, and P. Vettiger, Appl. Phys. Lett. **75**, 403 (1999).
[6] S. Y. Chou, P. R. Krauss, and L. Kong, J. Appl. Phys. **79**, 6101 (1996).
[7] M. Farhoud, H. I. Smith, M. Hwang, and C. A. Ross, J. Appl. Phys. **87**, 5120 (2000).
[8] H. Masuda and K. Fukuda, Science **268**, 1466 (1995).
[9] K. Liu, K. Nagodawithana, P. C. Searson, and C. L. Chien, Phys. Rev. B **51**, 7381 (1995).
[10] D. H. Pearson and R. J. Tonucci, Adv. Mater. **8**, 1031 (1996).
[11] H. Masuda, K. Yasui, and K. Nishio, Adv. Mater. **12**, 1031 (2000).
[12] S. Sun, C. B. Murray, D. Weller, L. Folks, and A. Moser, Science **287**, 1989 (2000).
[13] K. Liu, S. M. Baker, M. Tuominen, T. P. Russell, and I. K. Schuller, Phys. Rev. B **63**, 060403 (2001).
[14] V. F. Puntes, K. M. Krishnan, and A. P. Alivisatos, Science **291**, 2115 (2001).
[15] D. Weller and A. Moser, IEEE Trans. Magn. **35**, 4423 (1999).
[16] E. N. Abarra, A. Inomata, H. Sato, I. Okamoto, and Y. Mizoshita, Appl. Phys. Lett. **77**, 2581 (2000).
[17] E. E. Fullerton, D. T. Margulies, M. E. Schabes, M. Carey, B. Gurney, A. Moser, M. Best, G. Zeltzer, K. Rubin, and M. Doerner, Appl. Phys. Lett. **77**, 3806 (2000).
[18] D. A. Thompson, J. Magn. Soc. Jpn. **21**, 9 (1997).
[19] H. Katayama, S. Sawamura, Y. Ogimoto, J. Nakajima, K. Kojima, and K. Ohta, J. Magn. Soc. Jpn. **23**, 233 (1999).
[20] G. E. Thompson, R. C. Furneaux, G. C. Wood, J. A. Richardson, and J. S. Gode, Nature (London) **272**, 433 (1978).
[21] Calculated from the measured areas of the pores/dots, excluding those at the borders or those that appear to be touching due to the lack of contrast. The pores/dots, typically, with a 10%–20% eccentricity, are approximated as circles.
[22] J. Nogués, D. Lederman, T. J. Moran, and I. K. Schuller, Phys. Rev. Lett. **76**, 4624 (1996).
[23] M. R. Fitzsimmons, C. Leighton, J. Nogués, A. Hoffmann, K. Liu, I. K. Schuller, C. F. Majkrzak, J. A. Dura, J. R. Groves, R. W. Springer, P. N. Arendt, V. Leiner, and H. Lauter, Phys. Rev. B **65**, 134436 (2002).
[24] M. Grimsditch, Y. Jaccard, and Ivan K. Schuller, Phys. Rev. B **58**, 11539 (1998).
[25] B. D. Cullity, *Introduction To Magnetic Materials*, edited by M. Cohen (Addison-Wesley, London, U.K., 1972), Chap. 11.
[26] See, e.g. J. Nogués and I. K. Schuller, J. Magn. Magn. Mater. **192**, 203 (1999).
[27] P. J. Jensen, Appl. Phys. Lett. **78**, 2190 (2001).
[28] J. Sort, J. Nogués, X. Amils, S. Suriñach, J. S. Muñoz, and M. D. Baró, Appl. Phys. Lett. **75**, 3177 (1999).